Supplementary Information

A Novel Battery Separator Coated by a Europium Oxide/Carbon Nanocomposite Enhances the Performance of Lithium Sulfur Batteries

Lin Peng,[a] Zhanjiang Yu,[b] Mingkun Zhang,[a] Shunying Zhen,[a] Junhao Shen,[a] Yu Chang,[b,*] Yi Wang,[c] Yuanfu Deng,[d] Aiju Li [*a]

[a] School of Chemistry, South China Normal University, Guangzhou, 510006, China

[b] School of Environment, South China Normal University, Guangzhou, 510006, China

[c] Department of Mechanic and Electronic Engineering Zhongkai University of Agriculture and Engineering Guangzhou, 510225, China

[d] The Key Laboratory of Fuel Cell for Guangdong Province, School of Chemistry and Chemical Engineering, South China University of Technology, Guangzhou 510640, Guangdong, China

∗ Corresponding Author

*E-mail address: liaiju@scnu.edu.cn (A. Li), luckyu7704@163.com (Y. Chang)

Key words: Li-S batteries; Europium oxide; Oxygen-vacancy defect; Rare earth oxides; Catalyzing conversion

1. Experimental Section

1.1 Synthesis of Eu_2O_3/KB composite

Europium nitrate hexahydrate (Ⅲ) was purchased from Aladdin Reagent Co., Ltd., (Shanghai, China) and Ketjen Black EC600JD were obtained from MTI Corporation, China.. All chemical reagents were not further purified before use.

In the Synthesis process of Eu_2O_3/Ketjen Black (Eu_2O_3/KB), 120 mg KB was

firstly added into 50 ml absolute ethyl alcohol, followed by ultrasound dispersing for 2 h. Afterward, 3 ml of 0.1 mol L^{-1} europium nitrate hexahydrate (Ⅲ) was added into the above solution with magnetically stirring for 30 mins at room temperature. Then, the mixture was adjusted to achieve a pH value of 8.5 by adding ammonium hydroxide. Subsequently, the product was washed, centrifuged and dried at 60 ℃ for 10 h. After that, the product was calcined at 900 ℃ for 2 h under a nitrogen atmosphere.

1.2 Material characterizations

The crystal structure of Eu_2O_3/KB was examined by X-ray diffraction (XRD, Rigaku Ultima IV). The morphology and microstructure of Eu_2O_3/KB were analyzed by scanning electron microscope (SEM, ZEISS Ultra 55) and transmission electron microscope (TEM, FEI Talos F200X). Specific surface area of Eu_2O_3/KB and KB was carried out by Brunauer-Emmett-Teller method (BET, ASAP 2460). The Eu_2O_3 content in Eu_2O_3/KB composite was performed by thermogravimetric analysis (TG, NETZSCH TG 209 F3). Surface chemical characteristics of Eu_2O_3/KB was analyzed by X-ray photoelectron spectroscopy (XPS, AXIS SUPRA). The oxygen vacancy of Eu_2O_3/KB was detected by electron paramagnetic resonance (EPR, EMXPlus-10/12).

1.3. Preparation of Eu_2O_3/KB and KB-modified separator

Eu_2O_3/KB of 60 wt% and poly(vinylidene difluoride) (PVDF) of 40 wt % was uniformly dispersed in 1-methyl-2-pyrrolidinone (NMP) then coated on one side of a porous polypropylene separator (Celgard 2400). The slurry coated separator was dried at 60 ℃ for 12 h in a blast oven. Finally, the resulting Eu_2O_3/KB-modified separator (Eu_2O_3/KB/PP) was punched into circular disks with a diameter of 19 mm. For

comparison, KB-modified separator (KB/PP) was also fabricated above the analogously method. The areal loading of modified materials was ascertained about 0.22 mg cm^{-2}.

1.4 Symmetric cell test and absorption measurement

Symmetric cell test. Eu_2O_3/KB of 90 wt% and PVDF of 10 wt% were evenly dispersed in 1-methyl-2-pyrrolidinone (NMP) to prepare a slurry. The obtained slurry was coated on an aluminum foil and then dried at 60 ℃ for 12 h. The dried foil was punched to circular disks. Li_2S and S was mixed at a molar ratio of 1:5. A blank separator with two sides was injected to electrolyte of 0.05 M Li_2S_6 and bis(trifluoromethanesulfonyl)imide lithium (LiTFSI) in 1,3-dioxolane (DOL) and 1,2-dimethoxyethane (DME) (v/v=1:1) was assembled to cell in an Ar-filled glove box. The cells were carried out cyclic voltammetry (CV) at a scan rate of 5 mV s^{-1} in a voltage window of -0.6 to 0.6 V (vs. Li/Li^+).

Visual absorption experiment. Li_2S and S (a molar ratio of 1:5) was mixed up to 1.5 mM Li_2S_6 solution with in DOL and DME (v/v=1:1). The same specific surface area of Eu_2O_3/KB and KB was infiltrated in 1.5 mM Li_2S_6 solution with same volume. Afterwards, their supernatant solution is collected to detection for UV-Visible spectrum.

1.5 Preparation of electrodes and electrochemical measurements

Sulfur cathode preparation. The sulfur cathodes were prepared by mixing and grinding for 70 wt% sublimed S, 20 wt% acetylene black, 10 wt% PVDF and appropriate NMP in an agate mortar for about 30 min. Subsequently, uniform slurry

was coated on an aluminum foil and then dried at 60 ℃ for 12 h. the obtained sulfur cathodes was punched into circular disks with a diameter of 10 mm. The sulfur mass loading in the cathode is 1～7 mg cm^{-2}.

Electrochemical measurements. CR2032 coin cells were assembled in an Ar-filled glove box (O_2, H_2O <0.01 ppm) using lithium foils as anodes and Eu_2O_3/KB/PP, KB/PP and PP as separator. The electrolyte was 1 M LiTFSI in DOL and DME (v/v=1:1) with 0.1 M $LiNO_3$ as an additive. The discharge/charge performance tests of the assembled cells were evaluated by a Neware battery test system within a voltage window of 1.8-2.8 V (vs. Li/Li^+). The CV measurements at a scanning rate of 0.1 mV s^{-1} in voltage between 1.8-2.8 V (vs. Li/Li^+) and electrochemical impedance spectroscopy (EIS) tests with frequency range from 100 KHz to 0.01 Hz. The CV and EIS were measured by a CHI660E electrochemical workstation.

1.6 DFT Calculation

Computational Method. Density Functional Theory (DFT) derived from branch of First-principles calculations was employed to calculate adsorption energy. The calculation of DFT based LDA+U approach was performed by the VASP (Vienna AB-Initio Simulation Package) Package code. All the atoms involved were in fully released state with an energy convergence value of 5×10^{-5} eV. The vacuum layer was 15 Å. The internal vertical force reduced to below 0.05 eV/Å. The plane wave was set to an energy cutoff of 500 eV. Projector augmented wave (PAW) potential function and Perdew-Burke-Ernzerhof (PBE) versions of generalized gradient approximation (GGA-PBE) Exchange-correlation potential function were used to reveal ion and electron

interactions. A uniform K-point grid was adopted to collect the system energy. The van der Waals (vdW) interactions was corrected by Grimme semi-empirical DFT-D3 scheme. The adsorption energy of Li_2S_x (Li_2S_x, x=1,4,6,8) (E_{ads}) on Eu_2O_3 (222) facet was determined according to the following equation:

$$E_{ads} = E_{sub+s} - E_{sub} - E_s$$

Where E_{ads+s}, E_{sub} and E_s were the adsorbed energy of Li_2S_x-Eu_2O_3 (222) facet, substrate and Li_2S_x, respectively.

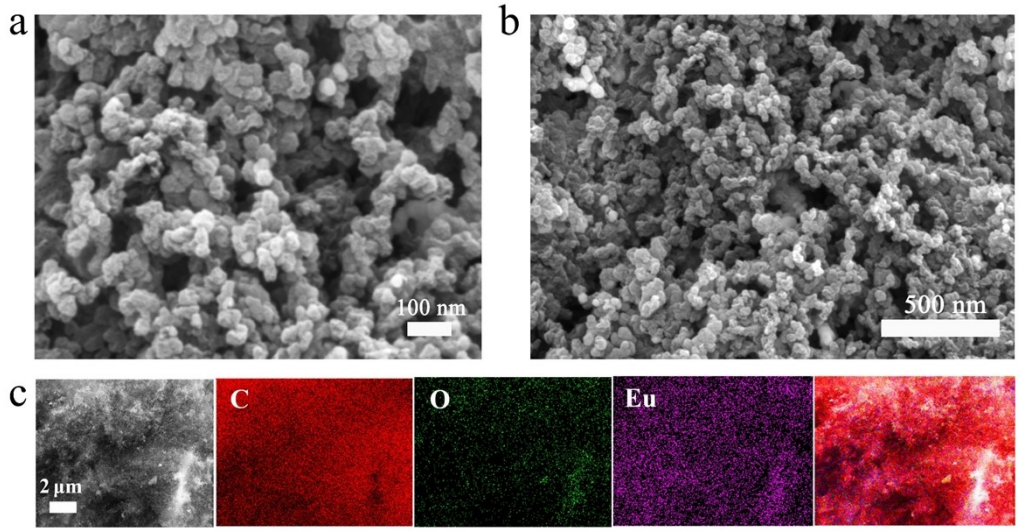

Fig. S1 (a-b) SEM images of Eu_2O_3/KB. (c) EDS elemental mapping images of Eu_2O_3/KB.

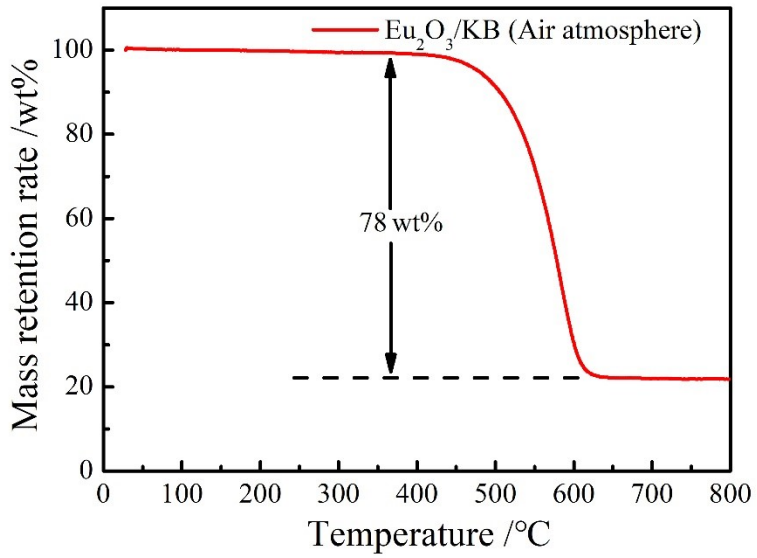

Fig. S2. The thermogravimetric curve of Eu_2O_3/KB at atmosphere.

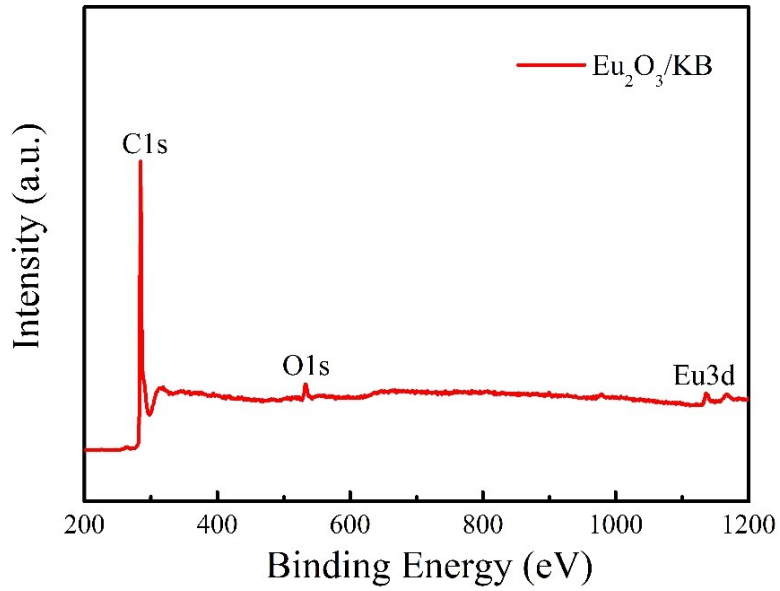

Fig. S3. XPS survey spectra of Eu_2O_3/KB.

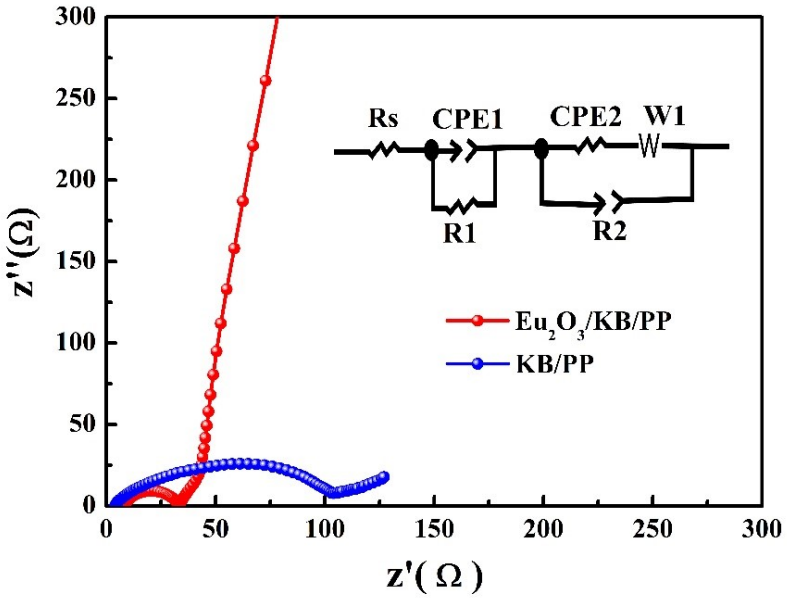

Fig. S4. The EIS spectra of KB/PP and Eu_2O_3/KB/PP after 500 cycles at 1 C rate.

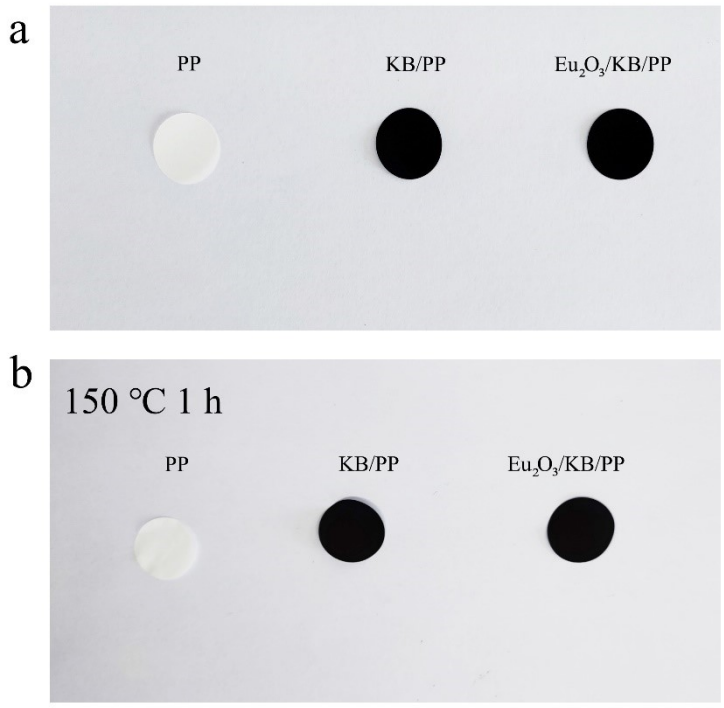

Fig. S5. Thermal stability tests of three separators.

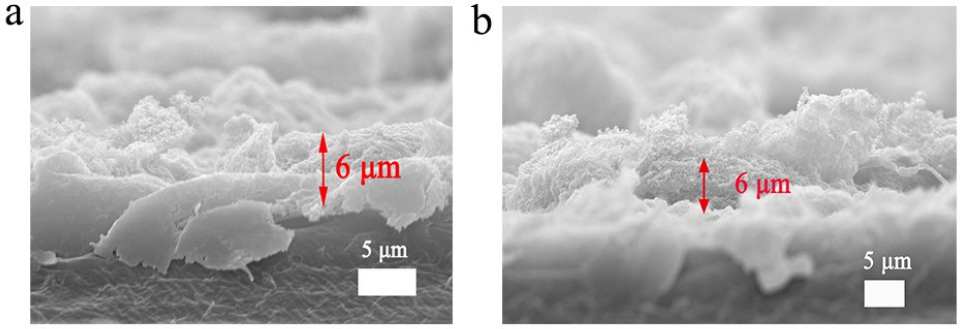

Fig. S6. The cross-sectional images of (a) the Eu_2O_3/KB/PP and (b) KB/PP separators.

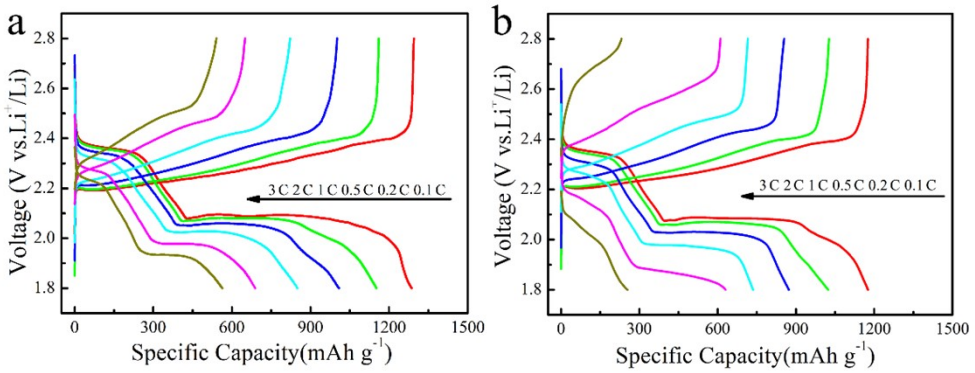

Fig. S7. GDC profiles of (a) the Eu_2O_3/KB/PP and (b) KB/PP at various current densities.

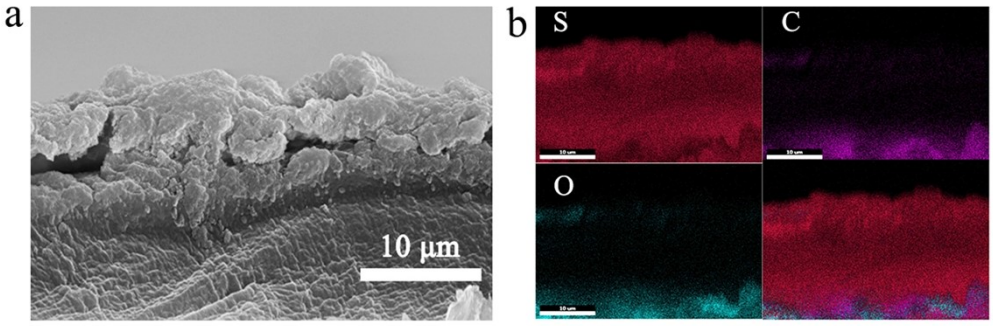

Fig. S8. The cross-sectional EDS elements mapping images of the KB/PP separator after 220 cycles.

Table. S1. Compared to electrochemical performance of modified commercial separator with rare earth oxides for Lithium sulfur batteries.

Modified-PP separators	**Cathode materials**	**Sulfur loading /mg cm^{-2}**	**Current density/C-rate**	**Initial discharge capacity /mAh g^{-1}**	**Discharge capacity /mAh g^{-1} (after n cycles)**	**Capacity decay rate per cycle (%)**	**References**
Eu_2O_3/KB/PP	**Pure S**	**2.2**	**0.2**	**951**	**757 (200)**	**0.11**	**This work**
Eu_2O_3/KB/PP	**Pure S**	**1.3**	**1**	**878**	**644 (500)**	**0.05**	**This work**
MWCNTs/CeO_2/PP	Pure S	1.8–2.0	0.2	898.3	≈520 (300)	0.14	[1]
S/KB-CeO2	S/KB	2	0.2	830	≈415 (500)	0.1	[2]
CeO_2@G	Pure S	1.2	≈0.6	1100	≈740 (300)	0.11	[3]
CeO_2/RGO	Pure S	2	0.1	1136	886 (100)	0.22	[4]
Sc_2O_3@CNT	CMK8-S	1.5	1	1037	788 (500)	0.48	[5]
Y_2O_3-KB	KB/S	1.296	1	1054	816 (200)	0.11	[6]
YHS/CNT-0.6	YHS@C/S	2.1	1	809.6	521.69 (500)	0.07	[7]

[1] W. Zhu, Z. Zhang, J. Wei, Y. Jing, W. Guo, Z. Xie, D. Qu, D. Liu, H. Tang, J. Li, J. Membr. Sci.,2020, **597**, 117646.

[2] L. Wu, Z. Wang, C. An, G. He, J. Alloy. Comp., 2019, **806**, 881-888.

[3] P. Cheng, P. Guo, K. Sun, Y. Zhao, D. Liu, D. He, J. Membr. Sci., 2021, **619**, 118780.

[4] S. Wang, F. Gao, Y. Zhao, N. Liu, T. Tan, X. Wang, Nanoscale Res. Lett., 2018,

13, 377.

[5] J. Xu, Q. Zhang, X. Liang, J. Yan, J. Liu, Y. Wu, Nanoscale, 2020, **12**, 6832-6843.

[6] S. Wang, X. Qian, L. Jin, D. Rao, S. Yao, X. Shen, K. Xiao, S. Qin, J. Solid State Electro., 2017, **21**, 3229-3236.

[7] P. Zeng, M. Chen, J. Luo, H. Liu, Y. Li, J. Peng, J. Li, H. Yu, Z. Luo, H. Shu, C. Miao, G. Chen, X. Wang, ACS Appl. Mater. Interfaces, 2019, **11**, 42104-42113.